Journal of Ceramic Processing Research. Vol. 25, No. 4, pp. 599~606 (2024)
(Received 11 March 2024, Received in revised form 5 June 2024, Accepted 7 June 2024)
https://doi.org/10.36410/jcpr.2024.25.4.599

J O U R N A L O F
Ceramic Processing Research

Physicochemical properties and antibacterial studies of hydroxyapatite scaffold extracted from indonesian limestone

Juliasih Partini[a], Silma Maula Bilqis[a], Fikri Addin Salimy[a], Ihwanul Aziz[b], Mona Sari[c], Nilam Cahyati[a] and Yusril Yusuf[a,*]

[a]*Department of Physics, Faculty of Mathematics and Natural Science, Universitas Gadjah Mada, Yogyakarta 55281, Indonesia*
[b]*Research Center of Accelerator Technology, Research Organization of Nuclear Energy, National Research and Innovation Agency (BRIN), Yogyakarta, Indonesia*
[c]*Department of Physics Education, Faculty of Mathematics and Natural Science, Universitas Negeri Yogyakarta, Yogyakarta 55281, Indonesia*

This research successfully fabricated scaffolds with hydroxyapatite (HA) from limestone and with HA coating using the gas foaming method. HA coating uses the addition of cinnamon oil in HA from limestone and impacts the scaffold's antibacterial properties. Scaffold fabrication uses the gas foaming method with a drying time of 30 minutes and 0.9 grams of HA. The fabricated scaffold is then characterized using an X-ray diffractometer (XRD), Fourier Transform Infra-Red (FTIR), and Scanning Electron Microscopy (SEM). Then, the antibacterial analysis of scaffolds using the diffusion method. Scaffolds from HA coating have smaller crystal sizes, fewer agglomerations, smaller particle sizes, and a more even distribution and size of pores. Scaffolds with HA coating have higher porosity than scaffolds with HA only. HA coating shows that adding cinnamon oil as an antibacterial agent can inhibit strong bacteria for *S. aureus* bacteria with an inhibition zone size of 11 mm.

Keywords: Limestone, Hydroxyapatite, Gas foaming, Scaffold, Antibacterial.

Introduction

Biomaterials are natural or synthetic, biocompatible materials that can be used in the medical world and interact with biological systems [1, 2]. Biomaterials have several requirements, including not hurting the body, having corrosion resistance, and having good strength. In its application, biomaterials are used to replace or restore the function of damaged bone components. The selection of biomaterials used as implants must meet several requirements, including biocompatible, bioactive, and osteoconductive. Biomaterials that are being and continue to be developed are hydroxyapatite and carbonate hydroxyapatite.

Hydroxyapatite (HA) or calcium hydroxyapatite is a type of apatite material with the chemical formula $Ca_{10}(PO_4)_6OH_2$ [3], which is often applied in the medical and dental fields [4, 5]. Hydroxyapatite is biocompatible, bioactive, osteoconductive, and non-toxic [6, 7]. HA, as a bioceramic in the medical field, has similarities to the mineral phase in bones and teeth, so it has bioactive biocompatibility properties that allow the surrounding tissue to grow into the implant as well as porosity so that a better bond with the tissue can be obtained [5, 6]. Hydroxyapatite was shown to be biocompatible and very well tolerated by human oral cavity tissues, has osteoconductive capabilities, and was shown to stimulate osteoblast differentiation and bone formation [6, 8, 9].

HA can be synthesized from biogenic materials such as shells, egg shells, cockle shells, fish bones, leaves, and plant stems [10, 11]. Limestone has enormous potential and is spread almost evenly throughout Indonesia. Limestone is widely used as an industrial raw material, cement, foundation stone, plaster for masonry mortar, and decorative stone. Limestone contains mainly calcium carbonate minerals, around 95%. The calcium carbonate content can be converted into calcium oxide by calcination so that it is easier to purify to obtain the calcium. Based on this potential, limestone was chosen as the primary material in the synthesis of hydroxyapatite.

HA powder can be synthesized using various reactants under different processing conditions, such as hydrothermal, sol-gel, precipitation, solid-state reaction, microemulsion, and mechanochemical [12-14]. The synthesis method chosen in this study is the precipitation method because the synthesis process is simpler, easier, does not require expensive reagents, is effective, and is able to get the desired CaP product results even though it depends on variables such as material composition, pH, stirring time, temperature, and others. HA is one of the materials used to make scaffolds [15, 16]. The

*Corresponding author:
Tel : +62-0274-6492383
Fax: +62-0274-6492383
E-mail: yusril@ugm.ac.id

scaffold is a three-dimensional structure that serves as a skeleton for bone growth. The scaffold quality is influenced by porosity, pore size distribution, and good interconnectivity. Scaffolds with high porosity will make it easy for cells to diffuse while carrying out life activities such as obtaining nutrients and oxygen. Micropores (<50 μm) in the scaffold function as a medium for protein exchange, ion exchange, and beekeeping of osteoblast cells. While macropores (>300 μm) function as a place for cell colony growth, nutrient transport, and metabolism [17]. A material can meet the candidate standard as a cancellous bone scaffold if it has a porosity of about 60-70% [18, 19].

The scaffold must also be safe and not contain impurities. Some things that can be done to maintain biocompatible properties in making scaffolds include using methods and mixed substances that are not contaminants. In scaffold synthesis, one method that can produce a reasonably high porosity scaffold is the gas foaming method. As for the advantages of this method, such as ease of use and cost-effectiveness, the resulting porosity is relatively high and does not produce residues [20]. The gas foaming method also uses a compound as a foaming agent to stimulate foam formation. Hydrogen peroxide (H_2O_2) has thermodynamic instability, so it quickly decomposes into H_2O and O_2. The advantage of hydrogen peroxide as a foaming agent is that it does not pollute the environment because all that is left is water and oxygen. The fabrication results are expected to have potent properties, wide surface pores, heat insulators, and low density [21].

One step that can be taken to increase the safety of the scaffold so that it is not toxic can be done by adding substances/polymer that have antibacterial abilities. Cinnamon oil has been used in traditional medicine for centuries and is known as a natural antibacterial and antioxidant [22]. Of the various essential oils, cinnamon essential oil has a wide range of functions such as anti-hyperglycemic, antidiarrheal agent, anti-hyperlipidemia, anti-toxin, anti-inflammatory, anti-lice, hepatoprotective, gastroprotective, antioxidant, antibacterial [23]. This essential oil has antibacterial content that is quite effective in dispelling the growth of bacteria and fungi. Cinnamon extract causes cell membrane damage in bacteria, as well as has an excellent antibacterial effect against S. *aureus* bacteria [24]. Therefore, manufacturing HA scaffold with gas foaming method and cinnamon oil is expected to provide benefits as an antibacterial.

Materials and Methods

Materials

The materials used in this research include limestone obtained from Rongkop, Gunung Kidul, Yogyakarta, Indonesia. Diammonium phosphate [$(NH_4)_2HPO_4$] and ammonium hydroxide (NH_4OH) 25%, produced by Merck, USA.

Methods

Synthesis of Hydroxyapatite (HA)

HAp synthesis was carried out using the precipitation method. An amount of 10 grams of calcium oxide (CaO) powder was dissolved in 100 ml of distilled water, then stirred using a hot plate magnetic stirrer at a speed of 350 rpm for 2 hours at a temperature range of 60°-70°C. Then, 14.13 grams of $(NH_4)_2HPO_4$ were dissolved in 100 ml of distilled water and stirred using a hot plate magnetic stirrer for 2 hours at a temperature range of 60°C-70°C. After 2 hours, the $(NH_4)_2HPO_4$ solution was titrated slowly into the CaO solution using a burette (dropwise) while still stirring. The mixed CaO and $(NH_4)_2HPO_4$ solution was then added with NH_4OH until the solution had a pH>9.5. After adding NH_4OH, the solution was stirred for 1 hour at a speed of 350 rpm at a temperature range of 60°C-70°C. The HA solution formed was allowed to stand (aging) for 24 hours to produce a precipitate. The precipitate remaining on the filter paper was taken and dried at 90°C for 6 hours. Then, the HA was calcined at 1000°C for 6 hours.

Synthesis of HA coating

The purpose of this process was a sample of hydroxyapatite covered with cinnamon oil as an anti-bacterial agent. A total of 3 grams of hydroxyapatite dissolved with 3 ml of 70% and 1 ml of cinnamon oil. Then, the mixture was stirred with a *stirrer* for 48 hours. The mixture results are dried in a vacuum oven at 60°C for 6 hours.

Fabrication of Scaffold

HA powder and HA coating were prepared in 0.9 grams each. Then, each HA and HA coating was mixed into 1 mL of H_2O_2 solution as a foaming agent. The mixture between those two materials was stirred for 2 hours. This process resulted in a semi-viscous solution

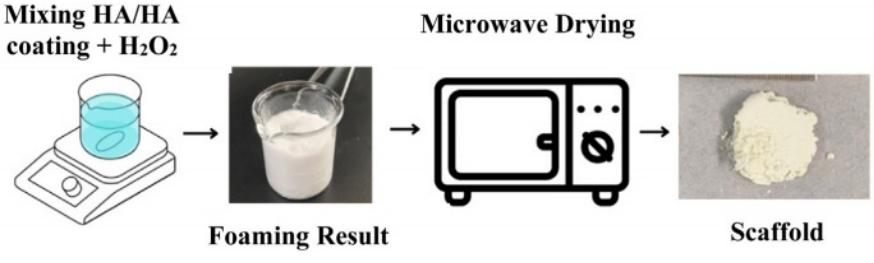

Fig. 1. Fabrication method of scaffolds.

with foam, which is continued with the heating process using a microwave with a power of 60P. Based on the *Sharp* R-26A0-900W microwave manual, the conversion of the value of 60 P in temperature units can be known from the formula:

$$\left(\frac{60}{100}\right) x\ 900 = 540\ Watt \quad (1)$$

In this microwave heating process, heating is carried out on a scale of 30 minutes for each HA and HA coating sample. After the drying process, two types of sample scaffolds can be obtained.

Physicochemical Characterization

X-Ray Diffractometer (XRD)

The results of the synthesis of HA were characterized using XRD to determine the crystal structure of the two materials. In XRD, the voltage is 40 kVolt, the electric current 30 mA, and a CuKα radiation source with a wavelength of 1.54 Å. Data was taken with a value of 2θ in the 3°-90°. The resulting data is in the form of intensity values at each 2θ angle formed. Then, the data is processed using the origin software into a curve to display the peaks resulting from diffraction. The parameters analyzed from the XRD diffraction patterns in this study include the calculation of lattice parameters, crystallite size, microstrain, and X-ray density.

Fourier Transform Infra-Red (FTIR)

The FTIR spectrophotometer was used to identify the functional groups of chemical compounds in HA and scaffold samples. FTIR data in the form of a spectrum is processed using origin software. Then, the results of FTIR data processing are analyzed by matching them to reference data.

Scanning Electron Microscope-Energy Dispersive X-Ray Spectroscopy (SEM-EDX)

SEM-EDX characterization aims to determine the morphology and Ca/P ratio for each sample. Additionally, analysis of the particle size distribution obtained from measuring 20-50 particles was also carried out.

Antibacterial Characterization

Antibacterial properties are the ability of a material to fight bacteria or the ability to inhibit the growth and development of bacteria. Materials that have these properties are commonly called antibacterial agents. This antibacterial agent is usually obtained naturally or from nature, or using artificial processes [24]. The mechanism of action of this antibacterial agent starts 42 from inhibiting the synthesis of bacterial walls that make the bacteria die due to lysis. Furthermore, it kills cells by damaging important cell membranes in bacteria. Antibacterials also inhibit protein synthesis by stopping protein synthesis by stopping the production of polypeptides, the latter of which can damage the replication system and repair of DNA from bacteria [25, 26].

The diffusion method was performed on HAp scaffold samples without antibacterial agents and scaffold samples with antibacterial agents. The bacteria used in this method is S. *aureus* which is one of the bacteria that live in bones and teeth [24] and *E. Coli*. The bacteria are diffused into agar in a petri dish. Then the scaffold sample that has been formed into a pallet is inserted into the bacterial dish. The next step is incubation for 24 hours. After incubation, samples in the tested petri dish will appear clear zones. This zone is an area where bacteria do not grow or thrive. This zone is called the inhibitory zone which indicates antibacterial activity [27]. This zone of inhibition is then measured as a parameter of antibacterial activity of the scaffold sample.

Results and Discussion

Characteristics of HA and HA coating

HA has a main diffraction pattern at position 2θ and index position hkl, respectively. The position is at 2θ 25,87°, 31,78°, and 32,90° with HKL index position (002), (211), and (300) according to references JCPDS 00-009-0432. The diffraction result is also used to determine the parameter values of the a and c grids. This lattice parameter is used to determine the c/a ratio. In addition, XRD analysis is also used to determine crystal size, microstrains, and crystallinity.

The XRD characterization results of limestone HA are shown in Fig. 2. Two diffractions are displayed: Fig. 2(a) is pure XRD HA diffraction, and Fig. 2(b) is XRD HA coating. Based on Fig. 2, the prominent diffraction peaks of pure HA are at 31,49° and HA coating at 31,68°. The peak value obtained is close to the reference HA value at JCPDS 00-009-0432, at position 2θ 31,77°. Pure HA from limestone has crystal size, lattice parameters, microstrains, and crystallinity, namely 56.64 nm, 0.73, 0.003, and 86.42%, respectively. Then, the HA coating obtained crystal size, parameter ratio, microstrain, and crystallinity of 50.117 nm, 0.73, 0.003, and 82.23%, respectively. It shows that there is

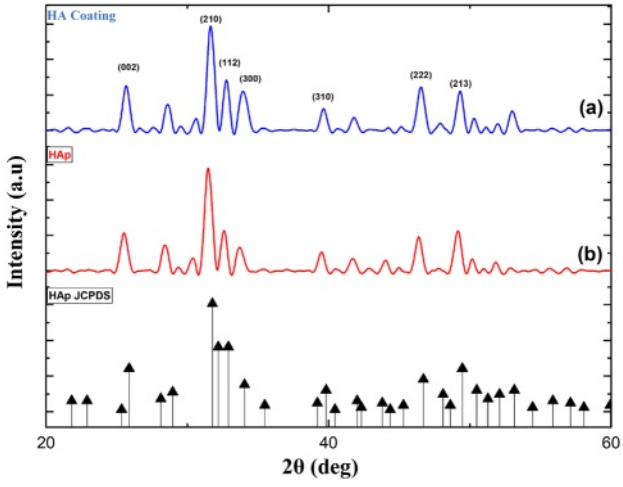

Fig. 2. XRD characterization: (a) HA coating and (b) HA.

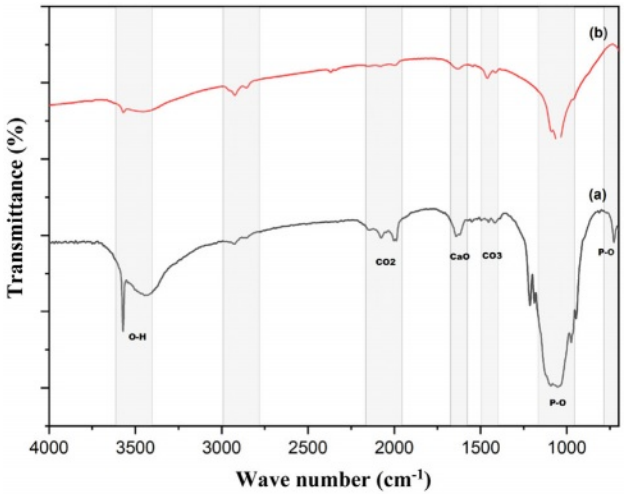

Fig. 3. FTIR Spectra: (a) HA, (b) HA coating.

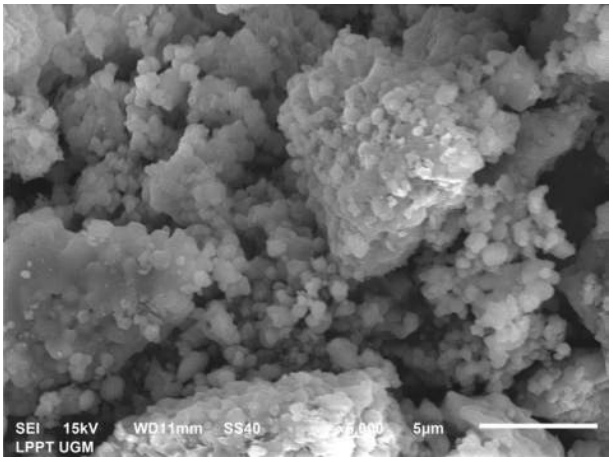

Fig. 4. SEM Image of HA.

no significant difference between pure HA and HA that has been coated with antibacterial agents.

Figure 3(a) shows the result of pure FTIR HA. The P-O bond group is shown at wavenumber 1049 cm^{-1} in pure HA. Sharp spectral peaks are also seen at wavenumbers 3448 cm^{-1} and 3573 cm^{-1}, indicating the presence of the O-H bond groups. Other peaks with lower intensity at wavenumbers 1416-1491 cm^{-1} indicate the presence of a C-O bond group. The CaO bond group appears at wavenumber 1623 cm^{-1}. The bond groups that appear are the constituent groups of the HA structure. The appearance and detection of these bond clusters indicate that HA synthesized from limestone was successfully carried out.

Figure 3(b) is the result of FTIR HA coating. It can be observed that there is a sharp valley of the spectrum at wavenumbers 1019 cm^{-1}-1095 cm^{-1}, which indicates the presence of a PO_4 bond group. The presence of peaks at wavenumbers 3570 cm^{-1} and 3443 cm^{-1} indicates an OH bond group. The difference that can be observed is that several peaks of the spectrum experience ramps, whereas, in FTIR, samples without peak coating are more visible than samples that have been coated. The CaO wavenumber in HA coating samples looks slower than HA samples without antibacterial agents and the CaO bond group. The effect of antibacterial agents reduces the carbonate ion bonding seen at some wavenumber points. However, it does not change the main component of the HA constituent bond group.

SEM characterization is carried out to determine the morphology of pure HA samples and HA coating. The results of this characterization data are in the form of photographic images. The particle size distribution using the Image J and Origin 2018 applications was analyzed to calculate particle size. Fig. 4 shows the results of the SEM characterization of HA samples.

Figure 4 shows the morphology of HA in the form of particles with slight agglomeration. The distribution of agglomerations looks relatively evenly distributed at almost all points. The morphology of the particles shows that some particles are relatively large, and some are small. This indicates that the HA sample has an inhomogeneous distribution of particles. The particle size distribution calculation analysis results show that the average particle size is 1.26 µm. The results of EDX analysis are carried out to determine the percentage of elemental composition. The molar ratio Ca/P of the sample can be calculated and shows a result of 1.67. This value is by the reference HA's stoichiometry molar ratio, indicating that the HA synthesis has been successful.

Physicochemical Characteristics of Scaffold

The results of the characterization of pure XRD HA scaffold and HA Coating scaffold can be seen in Fig. 5, which shows a line spectrum with fairly sharp peaks. Diffraction peaks indicate the formation of the HA phase in the scaffold. The pattern and angle of diffraction formed in each image correspond to the HA pattern JCPDS 00-009-0432 in position (002), (211), and

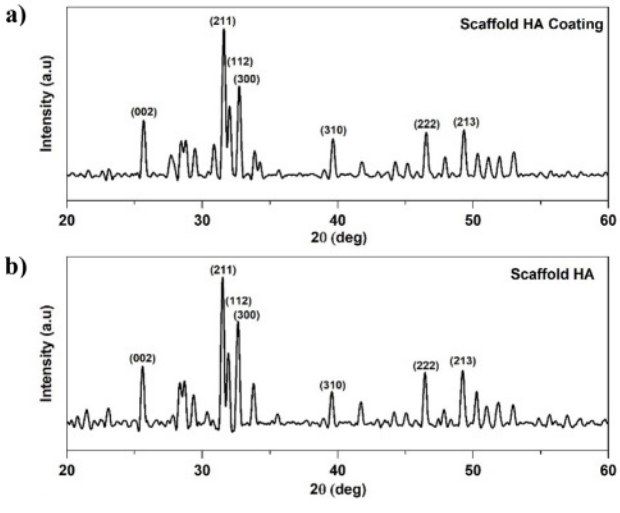

Fig. 5. XRD Patterns: (a) Scaffold HA Coating, (b) Scaffold HA.

Table 1. Crystal Size, Crystallinity, and Microstrain.

Sample	Crystal Size (nm)	a	c	c/a	Crystallinity	Microstrain
Scaffold Pure HA	59.06	9.50	6.96	0.73	79.14%	0.003
Scaffold HA Coating	56.308	9.48	6.94	0.73	78.27%	0.003

(300). Scaffold HA shows the highest peak at an angle of 31,45 °, 31,45 °, and 31,48 °. In the scaffold of the HA coating, the highest peak is at 31,56°, 31,59°, 31,98°.

The values of the grid parameters are shown in Table 1. The parameter ratio of the reference c/a grid is 0.73, and based on the data obtained, the whole data shows the same ratio of parameters as the reference. Microstrains in all samples showed a low number of 0.003. The results of this XRD characterization indicate that fabrication by the gas foaming method does not damage the HA structure inside the scaffold.

The crystallinity of pure HA scaffolds is 79.14%, and that of HA coating scaffolds is 78.27%. This indicates an influence of coating in the scaffold on crystallinity. Increased crystallinity indicates that the sample has improved crystalline quality. The size of the scaffold crystallite with variations in the amount of hydroxyapatite content shows that the crystal sizes have changed by 1 nm. The resulting sample size range is 51.06-58.38 nm. The crystal size of the HA coating scaffold tends to be smaller. Based on this, applying cinnamon oil as a coating impacts changing the size of smaller crystallites. Still, it does not damage the HA structure of the scaffold fabricated using the gas foaming method.

Figure 6(a) results from pure HA scaffold FTIR characterization. The effect of applying the foaming gas method with H_2O_2 as a foaming agent in pure HA scaffold fabrication can be seen from the FTIR results, which show consistent absorption in all samples in Fig. 6(a) with a wavenumber of 3572 cm^{-1}, which indicates the formation of an O-H group. Sharp absorption is also formed in the wavenumber range 960-1150 cm^{-1}, which is the functional group of P-O. Wavenumbers in the range 1400-1490 cm^{-1} indicate the presence of a

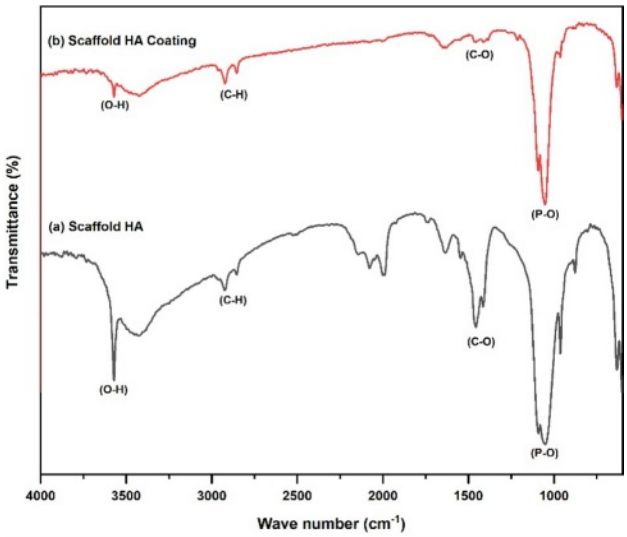

Fig. 6. FTIR Spectra: (a) Scaffold HA, (b) Scaffold HA Coating.

C-O group. The peak wavenumber between 1995 cm^{-1} and 2078 cm^{-1} marks the emergence of H_2O content. In addition, C-H group bonds appear at wavenumbers 2859 cm^{-1} and 2922 cm^{-1} with small intensity. This functional group arises due to several factors, including the emergence of additional contaminants during the sample fabrication process and experimental equipment contaminants.

The FTIR characterization of the HA coating scaffold is shown in Fig. 6(b). The results of FTIR analysis showed that the P-O functional group in the entire sample was at 1050-1100 cm^{-1}, while the O-H group was at wavenumber 3752 cm^{-1}. Hydrogen peroxide as a foam agent has no impact on the results of FTIR

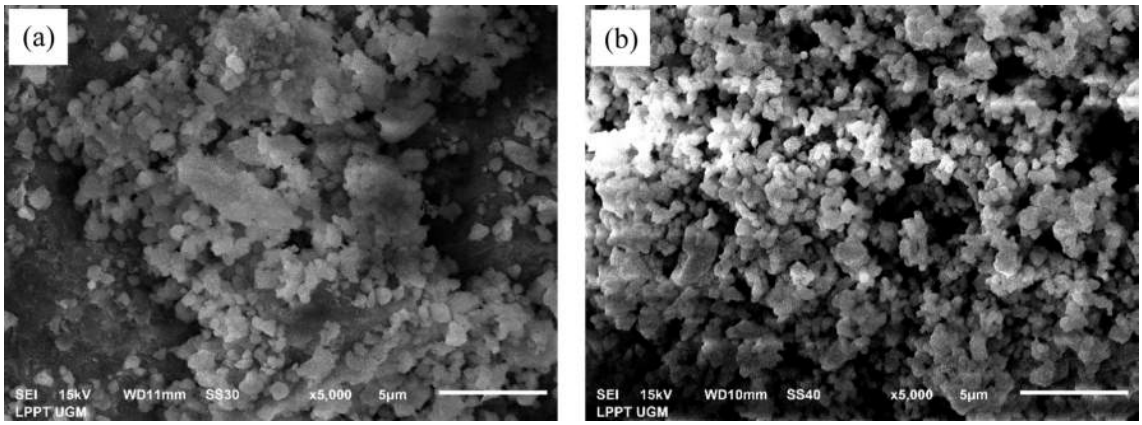

Fig. 7. SEM Images: (a) Scaffold HA (b) Scaffold HA Coating.

characterization. This is because the hydrogen peroxide mixed into the scaffold turns into H_2O and O_2 during stirring and dries when the scaffold is heated in the microwave. The previous research also shows the same result, namely, the results of scaffold fabrication using the gas foaming method have the advantage of not producing residue [28].

The main constituent groups of HA in the entire sample showed sharp intensity. The effect of adding antibacterial agents to the scaffold showed small peaks at wavenumbers 2800-2900 cm^{-1} throughout the sample, indicating symmetrical C-H uptake of cinnamon, as well as at wavenumbers 1620-1677 cm^{-1}, which is a coumarin aldehyde from cinnamon oil that appears in scaffolds. The HA functional groups, such as O-H and P-O groups, did not show significant changes between scaffolds without antibacterial agents and samples with antibacterial agents. Thus, adding an antibacterial agent of cinnamon oil in scaffold fabrication does not damage the constituent group of HAp and adds an antibacterial group in the FTIR characterization test.

Based on Fig. 7(a), the HA scaffold sample has an even agglomeration and distribution of particles. Analysis of particle calculations from HA scaffold samples shows that the sample has a particle size that is not too homogeneous, with a particle diameter size of about 0.28-1.88 μm. Its average particle size is (883 ± 11) × 10^{-3} μm. The analysis results showed that the pore size of the pure HA scaffold was in the range 0,6 - 1,952 μm. The average micropores in each variation of drying time of 20 minutes, 30 minutes, and 40 minutes are (508 ± 4) × 10^{-3} μm, (599 ± 5) × 10^{-3} μm, (477 ± 3) × 10^{-3} μm. The porosity of the HA scaffold from the SEM characterization obtained is 65%.

Figure 7(b) shows a sample of HA coating scaffold having less agglomeration and a more even distribution of particles. Analysis calculations showed that the HA coating scaffold sample had a particle size that was not

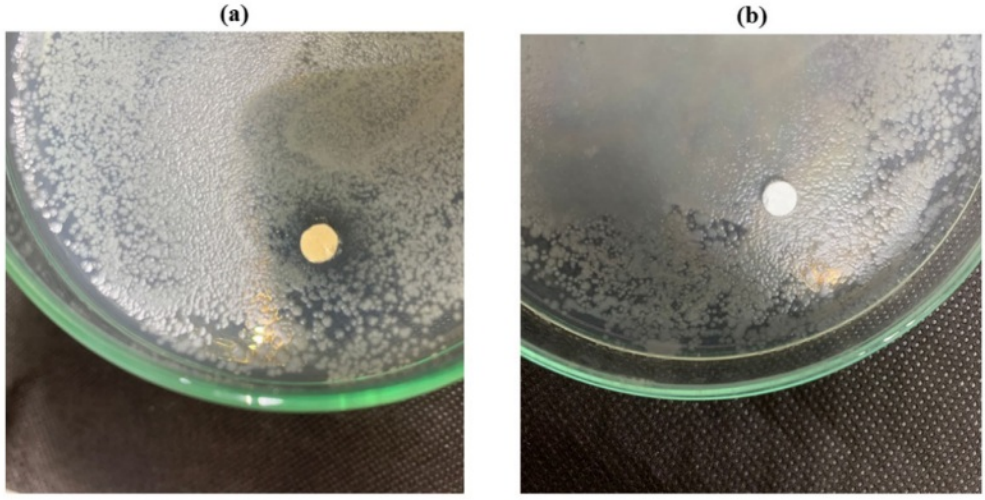

Fig. 8. Zone of Inhibition of *S. Aureus*: (a) Scaffold HA coating (b) Scaffold HA.

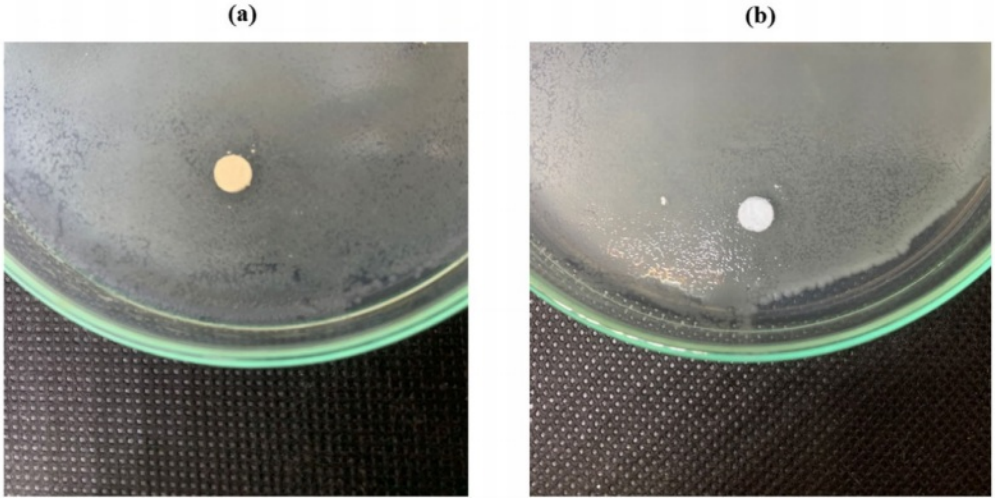

Fig. 9. Zone of Inhibiton of *E. Coli*: (a) Scaffold HA coating (b) Scaffold HA.

Table 2. Diameter of Zone of Inhibition.

Bacteria	Diameter	
	Scaffold HA Coating	Scaffold Pure HA
S. aureus	11 mm	0 mm
E. coli	0 mm	0 mm

too homogeneous, with a particle diameter size of 0.24-1.73 μm. The analysis showed that the HAp scaffold's pore size was 0.26-0.71 μm. The average micropores in the sample are $(52 \pm 9) \times 10^{-3}$ μm. The porosity of the HA scaffold obtained has a value of 71.33%.

Observation of the effect of adding antibacterial agents on the SEM characterization results shows that the HA coating scaffold has a more even distribution. Based on the calculation analysis, the average particle size of samples with antibacterial tends to shrink. HA-coating scaffolds' porosity has a higher average than scaffolds without antibacterial agents, with values of 69% and 67%. These results show that the porous scaffold was fabricated using gas foaming. The entire sample produces a morphology that is almost the same as the presence of aggregation. The results of the porosity analysis show that scaffold fabrication can be further investigated as a bone tissue engineering development.

Antibacterial Analysis of Scaffold

Analysis The antibacterial test was carried out using the diffusion method by measuring the diameter of the inhibition zone produced from the HA scaffold. Figure 8 is the antibacterial test result from pure HA scaffold samples and HA coating scaffolds using *S. aureus* bacteria. *S. aureus* bacteria are common causes of bone infections. Either from local trauma or surrogate tissue [29]. Tests were performed on scaffolds with pure HA and scaffolds with HA coating.

Test results for *S. aureus* bacteria showed that scaffold samples with antibacterial agents produced clear zones, indicating the presence of inhibitory zones in the test samples. The resulting inhibition zone has a diameter value of 11 mm, while pure HA scaffold samples show no clear zone, which means that this scaffold sample does not have an inhibitory zone. For testing using *E. coli* bacteria, data showed no zone of inhibition in either sample, which can be seen in Fig. 8.

The large diameter of the inhibition zone indicates the sample's ability to inhibit the bacterial growth rate. Table 2 shows scaffolds with antibacterial agents have an inhibition zone with a diameter of 11 mm, indicating this sample's inhibitory power is strong for *S. aureus* bacteria [30].

Conclusions

Pure HA from limestone and HA coated with cinnamon oil has been successfully synthesized. Scaffolds from HA coating have smaller crystal sizes, fewer agglomerations, smaller particle sizes, particle distribution, and pore sizes that are more even than scaffolds from pure HA. Antibacterial test results for scaffold HA coating on *S. aureus* bacteria showed strong antibacterial ability with an inhibition zone diameter value of 11 mm. Based on the results of physical-chemical properties and antibacterial tests that have been obtained, limestone HA coated with cinnamon oil can be the suitable alternative primary material for scaffold fabrication.

Acknowledgements

The authors are immensely grateful to the Faculty of Mathematics and Natural Science, Universitas Gadjah Mada, Yogyakarta 55281, Indonesia, through Collaborative Grant Program 2023 (No: 104/UN1/FMIPA.1.3/KP/PT.01.03/2023) and National Research and Innovation Agency (BRIN) through *Riset dan Inovasi untuk Indonesia Maju* (RIIM) 2023 (No: 30/IV/KS/05/2023) for financially supporting this research and publication. In addition, the authors would like to thank the Material Physics and Electronics Laboratory and the staff of the Integrated Laboratory for Research and Testing Universitas Gadjah Mada, Indonesia, for supplying the facilities and technical assistance.

Conflict of Interest Statement

The authors declare that they hold no competing interests.

References

1. Y. Yusuf et al., in "Karbonat Hidroksiapatit dari Bahan Alam: Pengertian Karakterisasi dan Aplikasi" (Gadjah Mada University Press, 2021) p. 4.
2. S. A. Doğdu, C. Turan, T. Depci, E. Bahçeci, K. Sangün, and D. Ayas, J. Ceram. Process. Res. 25[1] (2024) 85-91.
3. J.-H. Lee, H.-J. Choi, S.-Y. Yoon, B.-K. Kim, and H.-C. Park, J. Ceram. Process. Res. 14[4] (2013) 544-548.
4. J. Klinkaewnarong, S. Kamonwannasit, and P. Phatai, Chiang Mai J. Sci. 44[3] (2017) 1091-1099.
5. M. Sari, P. Henin, Chotimah, I.D. Ana, and Y. Yusuf, Mater. Today. Commun. 26 (2021) 1-12.
6. F. Thammarakcharoen and J. Suwanprateeb, Chiang Mai J. Sci. 47[4] (2020) 723-737.
7. L.A.F. Vieira, I.B. da C.J. Meireles, and E.M.B. Sousa, J. Ceram. Process. Res. 23[5] (2022) 725-736.
8. A. Yelten-Yilmaz and S. Yilmaz, Ceram. Int. 44[8] (2018) 9703-9710.
9. M.A. Roudan et al., J. Ceram. Process. Res. 18[9] (2017) 640-645.
10. M. Sari and Y. Yusuf, in Proceeding of the 1st Materials Research Society Indonesia Conference and Congress (Institute of Physics Publishing, 2018) p. 2.
11. Y. Rizkayanti and Y. Yusuf, Int. J. Nanoelectron. Mater. 11 (2018) 43-50.
12. C.M. Agrawal, J.L. Ong, M.R. Appleford, and G. Mani, in "Introduction to Biomaterials" (Cambridge University Press, 2014) p. 230.

13. V.J. Mawuntu and Y. Yusuf, in Proceeding of the 1st Materials Research Society Indonesia Conference and Congress (Institute of Physics Publishing, 2018) p. 1.
14. F.Y. Syafaat and Y. Yusuf, Int. J. Nanoelectron. Mater. 11 (2018) 51-58.
15. Y. Rizkayanti and Y. Yusuf, Int. J. Nanoelectron. Mater. 11 (2019) 85-92.
16. Al-Allaq, J.S. Kashan, M.T. El-Wakad, and A.M. Soliman, J. Ceram. Process. Res. 22[4] (2021) 446-455.
17. I.K. Januariyasa and Y. Yusuf, J. Asian Ceram. Soc. 8[3] (2020) 634-641.
18. N. Cahyati, M. Sari, and Y. Yusuf, ANSN. 15[3] (2024) 035004.
19. S. Panseri et al., J. Mater. Sci. Mater. Med. 32[1] (2021) 1-12.
20. L.A. García and M. Díaz, in "Cleaning in place" (Academic Press, 2011) p. 960-973.
21. A. Gunawan et al., SPECTA. J. Tech. 6[1] (2022) 8-24.
22. K. Wińska, W. Mączka, J. Łyczko, M. Grabarczyk, A. Czubaszek, and A. Szumny, Molecules. 24[11] (2019) 1-21.
23. S. Prabuseenivasan, M. Jayakumar, and S. Ignacimuthu, BMC. Complement. Altern. Med. 6[39] (2006) 1-8.
24. K. Wińska, W. Mączka, J. Łyczko, M. Grabarczyk, A. Czubaszek, and A. Szumny, Molecules. 24[11] (2019) 1-21.
25. H. Ullah and S. Ali, in "Antibacterial Agents" (InTech, 2017). p. 2.
26. M. Pirmoradian and T. Hooshmand, in "Applications of Nanocomposite Materials in Dentistry" (Elsevier, 2019) p. 237-269.
27. I. Gajic et al., MDPI. 11[4] (2022) 1-26.
28. S. Chung and T.J. Webster, in "Advances in Polyurethane Biomaterials" (Woodhead Publishing, 2016) p. 503-521.
29. E.A. Masters, B.F. Ricciardi, K.L. de M. Bentley, T.F. Moriarty, E.M. Schwarz, and G. Muthukrishnan, Nat. Rev. Microbiol. 20[7] (2022) 385-400.
30. D.J. Patty, A.D. Nugraheni, I.D. Ana, and Y. Yusuf, J. Biomed. Mater. Res. B. Appl. Biomater. 110[6] (2022) 1412-1424.